

PUSHOVER ANALYSIS OF GFRP PULTRUDED FRAMES

C. Casalegno^{1*} and S. Russo²

Keywords: GFRP pultruded frames, pushover analysis, overall ductility, GFRP pultruded joints

Results of a pushover analysis of GFRP pultruded frames aimed at the evaluation of their overall ductility are presented. It is assumed that the dissipation capacity of the frame structures is concentrated in joints due to their nonlinear behavior induced by progressive damage, while a brittle-elastic behavior is assumed for frame members. A two-storey one-bay GFRP pultruded frame is considered for a case study in which the column-base and beam-column joints are modeled with nonlinear rotational springs with different moment-rotation laws derived from experimental results available in the literature. For comparison, frames with hinged connections and moment-resisting frames are also analyzed. Finally, the results obtained are compared with those for a similar steel frame. The final results bear witness, in particular, to the absence of a significant ductility of pultruded frames and the relevant influence of the characteristics of bracings on their structural response.

1. Introduction

There is currently a great interest in the use of glass-fiber-reinforced polymer (GFRP) composites in civil engineering applications. This is due to their various advantages over traditional construction materials, such as, first of all, the high strength-to-weight ratio and durability [1].

In recent years, several large pultruded frame structures made of open-section GFRP profiles have been realized in the USA, the Southeast Asia, and Europe [2, 3]. A conscientious overall design of pultruded frame structures requires the definition of dynamic parameters to be used in seismic zones. The key feature of force-based seismic designs is the response modification factor (q or R), which is very widely employed to reduce the seismic accelerations to which the structures are subjected in consideration of their inelastic behavior [4]. This factor depends on the structural system, in which the type of material, the structural configuration, connections, the self weight, and boundary conditions simultaneously play an important

¹Ph.D., IUAV University of Venice, Dorsoduro 2206, 30123 Venice, Italy

²Associate Professor, IUAV University of Venice, Dorsoduro 2206, 30123 Venice, Italy

*Corresponding author; e-mail: carlo.casalegno@polito.it

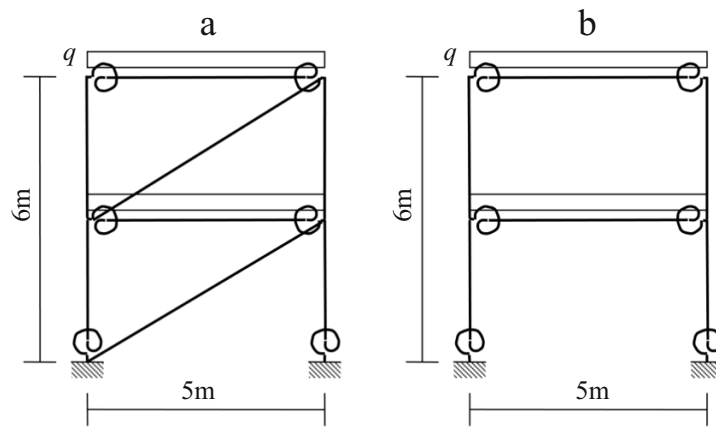


Fig. 1. Pultruded frames with (a) and without (b) bracings.

role [5-10]. The need for evaluating the overall ductility capacity of FRP structures, even if the material is brittle-elastic, is anyhow strategic.

A well-known method for evaluating the inelastic response of a structure to seismic actions, and then its ductility, is the pushover analysis, which consists in the application of increasing horizontal forces to the structure up to failure. The overall ductility is then evaluated on the base of the dissipation capacity induced by the nonlinear behavior of the structural system. Although many exploration have been carried out into the pushover analyses of steel and reinforced concrete structures (see [5-7, 9, 11-18] among others), the structural response of pultruded frames under horizontal actions has not been yet studied. In fact, although the study of the static behavior is now in-depth [2, 19-27] and some investigations have been already carried out on the evaluation of the elastic damping of pultruded members and structures [3, 28-30], a more in-depth study on the inelastic dynamic response is needed in order to define parameters for a seismic design. Indeed, even though the pultruded material is characterized by an elastic-brittle behavior, nonlinear and “pseudo-ductility” phenomena can be evidenced if attention is shifted from the material to the structure and its configuration through, first of all, the way of its assembly. In particular, the moment–rotation curves of bolted pultruded connections presented in this research points to a nonlinear behavior of the joints, as the load is increased up to failure, due to the progressive damage of the elements that form the connection.

The present work is part of a more wide research program, still in progress, addressed to the evaluation of the dissipation capacity of pultruded structures based on the analysis of both the local nonlinear behavior of joints [31] and the global behavior of pultruded frames under seismic actions. In particular, in the work described herein, an attempt is made to evaluate the overall ductility of FRP pultruded frame structures by carrying out the pushover analyses of pultruded frames and assuming that the dissipation capacity of the structure is concentrated in its joints (as in timber structures), due to their nonlinear behavior induced by the progressive damage. That is to say, the dissipation capacity is devolved on the progressive damage mechanisms of the elements that form the connection and not to yielding of the material, since the pultruded material behaves linearly elastically up to failure. Results relative to experimental or numerical investigations into the inelastic response of pultruded structures subjected to horizontal actions have not been reported in the literature, to the best of knowledge of present authors. Only tests on pultruded frames subjected to short- and long-term vertical loads have been carried out [32, 33]. In our work, a two-storey one-bay GFRP pultruded frame is analyzed in detail. The column-base and beam-column joints are modeled by nonlinear rotational springs, while a brittle-elastic behavior is assumed for structural elements. For comparison, frames with hinged connections and moment-resisting frames are also analyzed. The final results are compared with those for a similar steel frame.

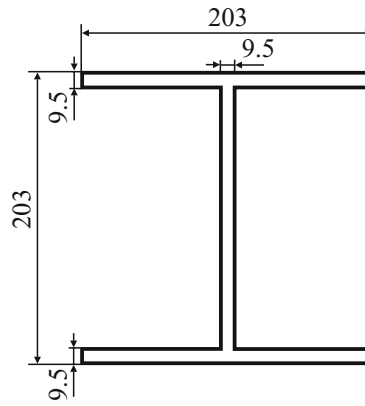


Fig. 2. Cross section of beams and columns employed in the pultruded frame (dimensions in mm).

2. Analysis of Pultruded Frames

The two-storey one-bay GFRP plane frame shown in Fig. 1 has been analyzed numerically. The frame is 6 m high, and its span is 5 m.

The frame is subjected to a distributed vertical load $q = 0.3$ N/m acting on its beams and to the self weight (1880 kg/m³).

The analysis is carried out on a two-dimensional model. Anyway, if the frame considered is supposed to have a regular shape in plan and elevation, this simplifying assumption does not have a significant influence on the modeling of its structural behavior. In fact, Eurocode 8 provisions [4] allow one to carry out a two-dimensional analysis of structures that satisfy the criteria of regularity.

The columns and beams are modeled by beam elements (L6BEN), taking into account the shear strain. Bracings are modeled by truss elements (L4TRU). Rotational springs (SPIRO) with nonlinear moment–rotation relations are used to model the column-base and beam-column joints [34].

The beams and columns have wide-flange sections of dimensions $203 \times 203 \times 9.5$ mm (Fig. 2). Different areas for the cross section of bracings are considered, and, with the aim of comparison, a frame without bracings is also analyzed (Fig. 1b).

A linear-elastic behavior is assumed for the beams and columns [35, 36]. The different behavior of bracings in tension and compression, induced by their buckling, is taken into account postulating a nonlinear behavior for their material, characterized by a negligible stiffness in compression. Two values for the ultimate tensile strength σ_u of bracings, 240 and 400 MPa, are considered in the analyses. The characteristics of the structural elements that form the pultruded frames considered in the analysis are reported in Table 1 together with their material properties.

The nonlinear moment–rotation relations for the pultruded joints are taken from the experimental results available in the literature. In regard to beam–column joints, the results of several experimental campaigns have been reported. A wide review work of tests on beam-column joints have been carried out in [37-38]. Pertaining column-base joints, on the contrary, the only tests reported in the literature, to our knowledge, are those carried out in [39].

In the present work, two different moment-rotation relations for column-base joints are considered, which were obtained from the experimental results and analytical formulations reported in [39]. In particular, the moment–rotation relations used in the FE model were found through the use of the formula

$$\Theta = \frac{M}{k_{ini} \left[1 - \left(\frac{M}{M_u} \right)^n \right]^{1/n}}, \quad (1)$$

TABLE 1. Characteristics of Structural Elements

Structural element	Cross section	Material behavior	Elastic constants, GPa		Ultimate strengt σ_u , MPa
			E	G	
Beams and columns	203×203×9.5 mm	Linear elastic	25	3	240
Bracings	0/5/10/20/40 cm ²	Nonlinear with a low stiffness in compression	25	—	240/400

TABLE 2. Characteristics of Joints [1-2]

Joint	Joint type	k_{ini} , kN · m/rad		M_u , N · m		Θ_u , rad
		Eq. (1)	Experiment	Eq. (1)	Experiment	
TC1	Column-base	1190	1330	4854	5720	0.024
TC2	Column-base	323	360	1515	1660	0.048
M1	Beam-column	-	94	-	1720	0.039

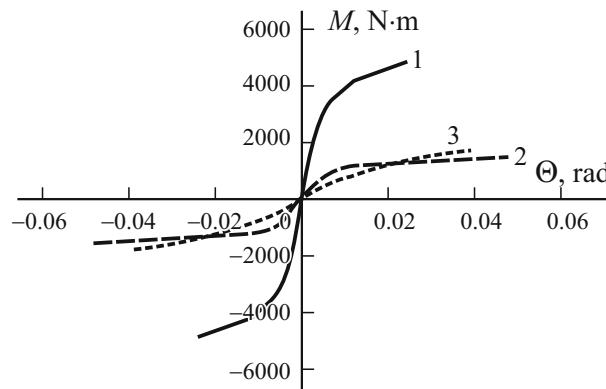


Fig. 3. Moment–rotation relations M – Θ for the TC1 (1), TC2 (2), and M1 (3) joints.

reported in the paper cited, where Θ is the rotation angle of joint, M is the applied bending moment, k_{ini} is the initial stiffness of joint, M_u is the ultimate bending moment of joint, and n is assumed equal to 1 (as suggested in the paper mentioned). The values of k_{ini} and M_u used in Eq. (1) to trace the moment–rotation diagram were obtained from the experimental tests reported in the paper cited.

The moment–rotation relation used for the modeling of beam-column joints is given in [37] as values of the rotational stiffness for increasing values of the bending moment applied.

The characteristics of joints are reported in Table 2, and the moment–rotation relations for three joints are represented in Fig. 3. The Turvey & Cooper CBL1 column-base joint (TC1 in what follows) is a web- and flange-cleated connection, which is characterized by the highest values of initial stiffness and ultimate bending moment and by the lowest value of the ultimate rotation angle. The Turvey & Cooper CBL3 base-column joint (TC2 in what follows) is only web-cleated and has an initial stiffness and a bearing capacity that are approximately 70% lower, but an ultimate rotation capability twice that of the former joint. The Mottram 1 beam-column joint (M1 what follows) is a web-cleated connection with characteristics close to those of joint TC2.

Looking at Table 2, it can be noticed that the initial stiffness and the ultimate bending moment of column-base joints computed by Eq. (1) (columns 3 and 5 of the table) are slightly underestimated relative to the experimental values (columns 4 and 6 of the table) reported in [39].

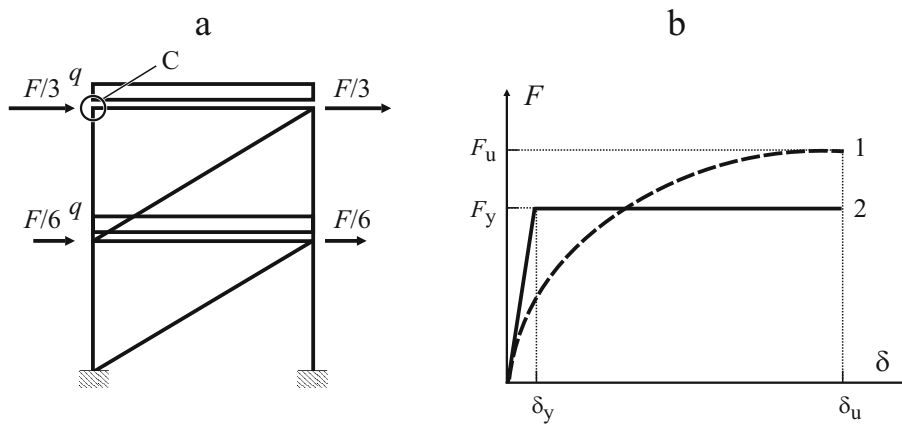


Fig. 4. Pushover analysis setup (a) and the idealized (1) and actual (2) response curves for evaluating the overall ductility (b).



Fig. 5. Brittle failure of timber bracings (a) and ductile collapse of steel bracings (b).

3. Pushover Analysis

The pushover analysis is a well-known approach to evaluating the overall ductility of structural systems [5, 9, 12, 13, 15, 17, 18]. It consists in a nonlinear analysis of a structure subjected to horizontal forces, usually linearly increasing with height or having magnitudes scaled with respect to the first vibration mode, as shown in Fig. 4a, where F represents the total applied horizontal force (i.e., the seismic base shear force). The horizontal forces are increased up to failure, and the overall ductility is evaluated idealizing the actual response curve. This curve represents the displacement δ of a control point (usually the top of the roof) in relation to the applied horizontal force F , as a curve relative to an elastoplastic oscillator with a single degree of freedom equalizing the areas subtended to the actual and idealized curves (Fig. 4b).

The overall ductility μ is computed as the ratio between the ultimate displacement δ_u at which failure of the structure occurs and the displacement δ_y at which the yield point is reached in the idealized curve (i.e., in the curve relative to the elastoplastic oscillator):

$$\mu = \delta_u / \delta_y. \quad (2)$$

The pultruded frames shown in Fig. 1 were subjected to horizontal forces linearly increasing with height (see Fig. 4a). The forces were increased up to failure. The geometric nonlinearities were also taken into account in the analyses. Failure of

TABLE 3. Analysis Results Relative to Those for the First Frame

S, cm^2	$k_{ini}, \text{kN/cm}$	F_{u^*}, kN	$\delta_{1,u^*}, \text{cm}$	$\delta_{2,u^*}, \text{cm}$	$\delta_{3,u^*}, \text{cm}$	$\delta_{4,u^*}, \text{cm}$	Collapse mechanism	μ
Frame without bracings (F1)	0.2	2	14.6	14.6	6.0	6.0	Ultimate rotation of beam-column joint	2.36
5 (F2)	9	110	12.3	12.1	7.0	6.6	Ultimate tensile strength of bracings	—
10 (F3)	16	192	11.6	11.4	6.7	6.1	—	—
20 (F4)	27	270	9.3	9.0	5.4	4.6	Ultimate rotation of beam-column joint	—
40 (F5)	43	314	6.7	6.3	3.9	2.9	—	—

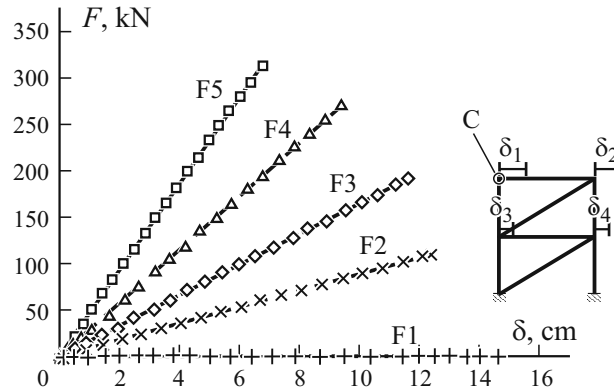


Fig. 6. Pushover curves $F-\delta$ of the first frame without bracings (F1) and with 5- (F2), 10- (F3), 20- (F4), and 40-cm² (F5) bracings.

a frame can occur by buckling instability, by reaching the ultimate rotation of joints, or by attainment of the ultimate strength of structural members.

It is assumed that the dissipative zones in the analyzed pultruded frames are located in joints, which is confirmed by many experimental results available in the literature (see [39-42] among others), while the beams and columns are regarded as behaving elastically up to failure. This condition is also assumed following the provision given by Eurocode 8 [4] for timber structures. In fact, the behavior of a GFRP frame can be regarded as similar to that of a timber frame, in which a brittle-elastic behavior is assumed for the structural members themselves, and the dissipation capacity is devolved to the nonlinear behavior of connections (as distinct from steel frames, in which the tensile bracing members are ductile elements and are expected to develop gross section yielding in a ductile manner). In Fig. 5, examples of the brittle failure of a timber bracing (Fig. 5a) and of the ductile collapse of a steel bracing (Fig. 5b) are illustrated.

4. Analysis Results

4.1. Frames with a nonlinear behavior of connections

The first frame analyzed is supposed to be realized through connection TC1 at the base of columns and connection M1 between beams and columns. The ultimate tensile strength of the structural members is 240 MPa.

For the frame without bracings and for frames with bracings of different dimensions, results of the analyses are reported in Table 3, and the pushover curves are shown in Fig. 6. As expected, the stiffness and the ultimate load-carrying

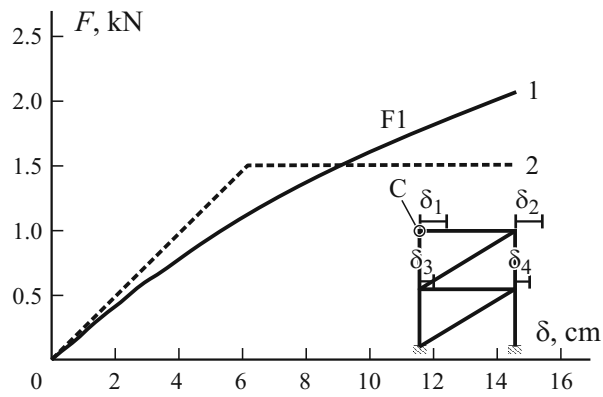


Fig. 7. Actual (1) and idealized (2) pushover curves of the first frame without bracings.

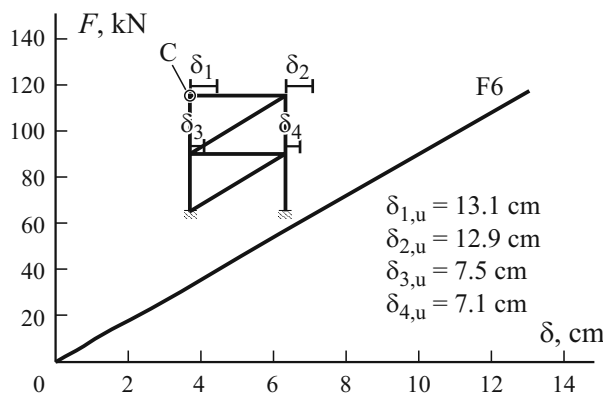


Fig. 8. Pushover curve of the first frame with 5-cm² bracings and an ultimate tensile strength of 400 MPa.

capacity of the frames, with respect to the horizontal forces, grow significantly as the cross section of bracings is increased, but the corresponding ultimate horizontal displacement decreases. So, with more stiff bracings, the hierarchy of different types of collapses moves from them to the failure of connections, which fail when the ultimate rotation in the beam-column joint is reached. Only the frame with 5-cm² (curve F2) bracings fails because of achievement of their ultimate tensile strength, namely when the lateral displacement at the roof level reaches 12 cm.

From the diagrams of Fig. 6, it can be seen that the behavior of the frames is linearly elastic up to failure. A slightly nonlinear behavior can be seen only for the frame without bracings (curve F1) if the diagram of the curve is enlarged (Fig. 7). In this case, the overall ductility $\mu = 2.36$. Nevertheless, the ultimate load-carrying capacity and stiffness of this frame with respect to horizontal forces are extremely low. As a consequence, bracings are required to guarantee the necessary stiffness and resistance, at least in the case of seismic actions.

A higher tensile strength, equal to 400 MPa, for the bracings was also considered in the analysis of the frames. Anyway, due to the failure by achievement of the ultimate rotation of joints, the results were exactly the same for the frames with 10-, 20- and 40-cm² bracings. In Fig. 8, the pushover curve for the frame with 5-cm² bracings, with an ultimate tensile strength of 400 MPa, is represented. In this case, failure occurs by reaching the ultimate rotation of beam-column joint. The ultimate load-carrying capacity and the ultimate displacement of the frame are slightly higher than those of the frame with less resistant bracings, while the behavior of the frame is still linearly elastic up to failure.

The second frame analyzed is supposed to be realized through the less stiff connection TC2 at the base of the columns and still with joint M1 between beams and columns. The ultimate tensile strength of structural members is again 240 MPa.

TABLE 4. Analysis Results Relative to Those for the Second Frame

S, cm^2	$k_{ini}, \text{kN/cm}$	F_u, kN	$\delta_{1,u}, \text{cm}$	$\delta_{2,u}, \text{cm}$	$\delta_{3,u}, \text{cm}$	$\delta_{4,u}, \text{cm}$	Collapse mechanism	μ
Frame without bracings (F1)	0.1	0.3	8.9	8.9	4.1	4.1	$P-\Delta$ instability	4.03
5 (F2b)	8	106	12.1	11.9	7.0	6.7	Ultimate tensile strength of bracings	—
10 (F3b)	16	200	12.2	11.9	7.2	6.5	Ultimate rotation of beam-column joint	—
20 (F4b)	27	281	9.7	9.4	5.7	4.8	" "	—
40 cm^2 (F5b)	43	324	7.0	6.6	4.1	3.0	" "	—

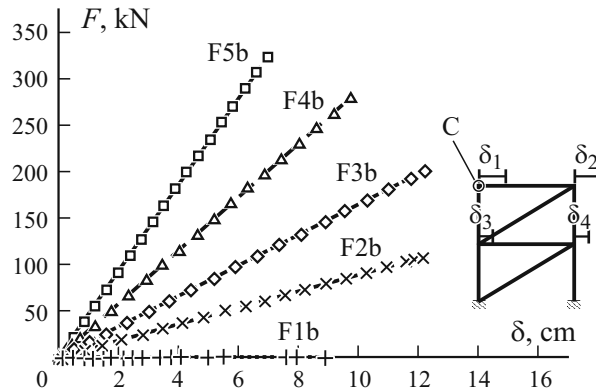


Fig. 9. Pushover curves $F-\delta$ of the second frame without bracings (F1b) and with 5- cm^2 (F2b), 10- cm^2 (F3b), 20- cm^2 (F4b), and 40- cm^2 (F5b) bracings.

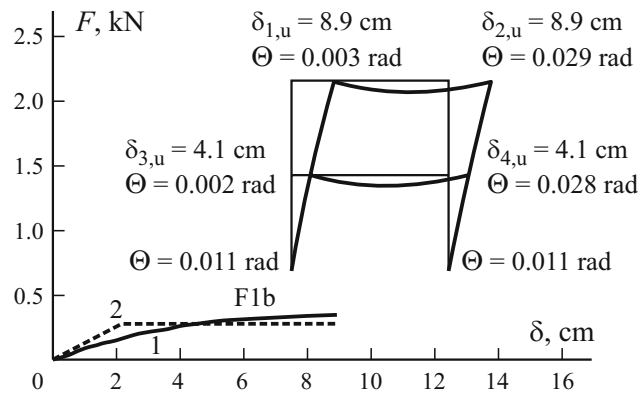


Fig. 10. Actual (1) and idealized (2) pushover curves of the second frame without bracings.

For the frame without bracings and for frames with different dimensions of bracings, results of the analyses are reported in Table 4, and the pushover curves are shown in Fig 9. In this case too, increasing the cross section of bracings, higher values of the stiffness and ultimate bearing capacity with respect to the horizontal forces are obtained, while the ultimate horizontal displacement is lower. The stiffness and resistance are lower than those of the first frame due to the lower stiffness of column-base connection. The behavior of the frames is linearly elastic up to failure, except for the frame without bracings (curve F1b). The actual and idealized pushover curves of this frame are represented in Fig. 10 together with its deformed shape at the last load step. The frame shows a nonlinear behavior and an overall ductility $\mu = 4.03$. Failure of the frame is due to the $P-\Delta$ instability. In fact, as indicated in Fig. 10, the rotation angle Θ of the joints at the last load step is smaller than the ultimate one.

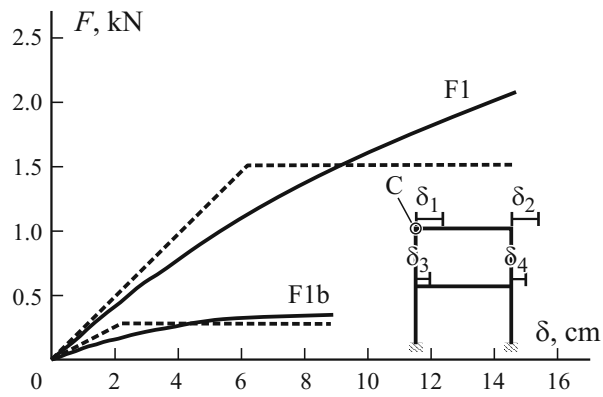


Fig. 11. Comparison of the actual (—) and idealized (---) pushover curves of the first and second frame without bracings.

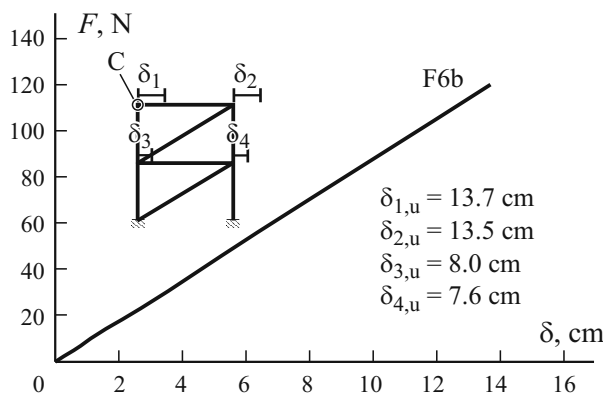


Fig. 12. Pushover curve of the second frame with 5-cm² bracings and an ultimate tensile strength of 400 MPa.

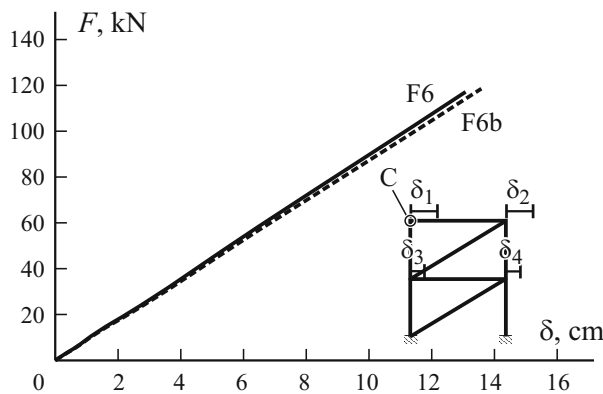


Fig. 13. Comparison of the pushover curves of the first (F6) and second (F6b) frames with 5-cm² bracings and an ultimate tensile strength of 400 MPa.

In Fig. 11, the pushover curves of two pultruded frames without bracings (curves F1 and F1b) are compared. A great difference between the stiffnesses and bearing capacities of the frames with respect to the horizontal actions, due to different characteristics of the column-base joints TC1 and TC2, is seen to exist.

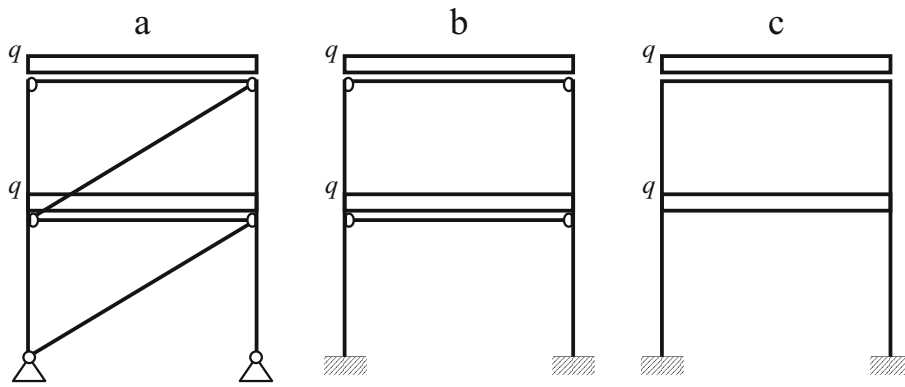


Fig. 14. Frame with hinges (a), frame fully restrained at the base (b), a continuous frame (c).

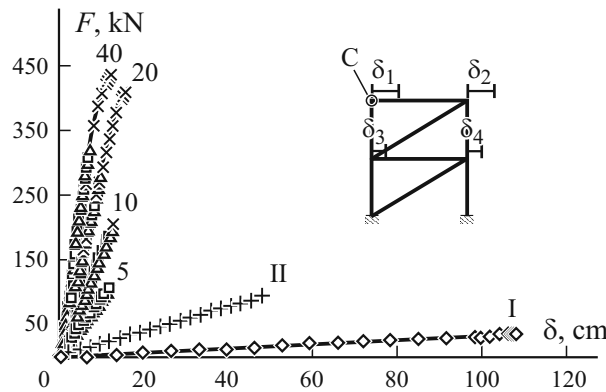


Fig. 15. Comparison between the pushover curves of frames with the nonlinear TC1 (\square) and TC2 (Δ) connections of a hinged frame (x) with different dimensions of bracings, of a frame fully restrained at the base (I), and a continuous frame (II).

For this frame, an ultimate tensile strength of 400 MPa for bracings was also considered. As for the first frame, the results are exactly the same as for the frames with 10-, 20-, and 40-cm² bracings, because the ultimate strength of the bracings is not reached. In Fig. 12, the pushover curve for the frame with 5-cm² bracings having an ultimate tensile strength of 400 MPa is represented. In this case, as for the first frame, the failure is caused by the ultimate rotation of beam-column joint. The ultimate load-carrying capacity and the ultimate displacement of the frame are slightly higher than those of the frame with less resistant bracings. The behavior of the frame is still linearly elastic up to failure.

In Fig. 13, the pushover curves for the first and the second frame with 5-cm² bracings and an ultimate tensile strength of 400 MPa (curves F6 and F6b) are compared. The behavior of the frames is very similar. The second frame is slightly less stiff with respect to the horizontal forces due to the lower stiffness of the column-base joint.

4.2. Hinged and moment-resisting frames

Analysis results for two frames having bracings with different cross-sectional dimensions were compared with those for a frame with the same characteristics, but with hinges instead of the nonlinear springs (Fig. 14a). Also, two moment-resisting frames were analyzed — one with hinges in the beam-column joints and fully restrained at the base (Fig. 14b) and the other with fully restrained joints (continuous frame, Fig. 14c).

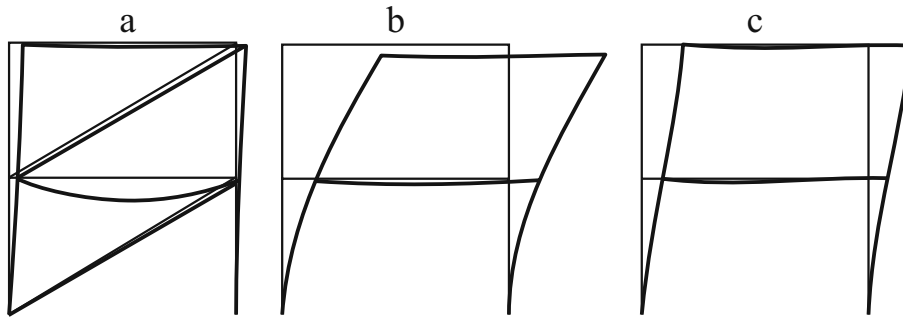


Fig. 16. Deformed shapes at the last loading step of a hinged frame with 40-cm² bracings (a), of a frame fully restrained at the base (b) and the continuous frame (c).

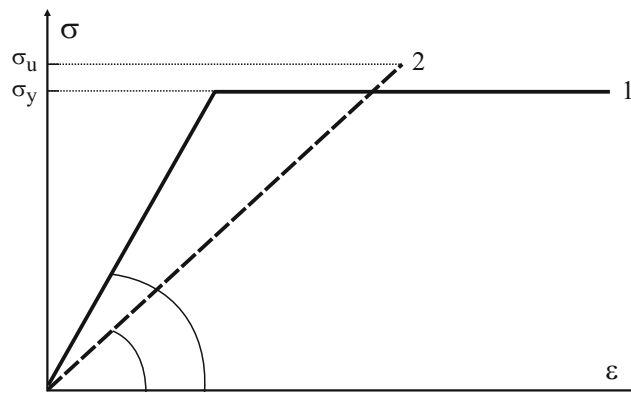


Fig. 17. Qualitative stress–strain diagram σ – ε of an elastic-ideally plastic material (1) and a GFRP pultruded material (2).

The correspondent pushover curves are shown in Fig. 15. As seen, the stiffness of the frames with a nonlinear behavior of connections with respect to the horizontal actions is the same as of a similar frame with hinges in the corresponding joints, i.e., without any rotational stiffness of the joints. Besides, disregarding the rotational capacity of joints in the hinged frame, the failure occurs due to achievement of the ultimate tensile strength of bracings in the case of the frames with 5-, 10-, and 20-cm² bracings, while the frame with 40-cm² bracings fails due to achievement of the ultimate bending moment of the corresponding first-floor beam. The ultimate displacements δ of the hinged frames are greater than those of the frames with nonlinear springs in the corresponding joints. The final nonlinear branch observed for the hinged frame with 40-cm² bracings (and, to a lesser extent, for the frame with 20-cm² bracings) is due to the initiating of buckling of the first-floor beam. In Fig. 16a, where the deformed shape of the frame with 40-cm² bracings at the last load step is illustrated, a significant flexural deformation of the first-floor beam is seen, which means buckling. The 40-cm² bracings, due to their high stiffness, act as restraints to the lateral displacement of the right side of the frame, and the beams are compressed, as evidenced by the difference between the lateral displacements of the left and right sides of the frame corresponding to the first-floor beam. In Fig. 16b-c, the deformed shapes of the frame fully restrained at the base (Fig. 16b) and of the continuous frame (Fig. 16c) are also represented. For the moment-resisting frames, it is assumed that a brittle-elastic failure occurs when the ultimate bending moment is reached in the corresponding base of the columns (the point of the maximum bending moment). The stiffness of those frames is much lower than of the other ones, while the ultimate displacement is much greater. Their behavior is linearly elastic up to failure.

TABLE 5. Material Characteristics of Structural Elements

Structural element	Cross section	Material behavior	E , GPa	σ_y , MPa
Beams and columns	HE120A	Elastic-ideally plastic	210	240
Bracings	2/5/10/20 cm ²	Elastic-ideally plastic with a low stiffness in compression	210	240

TABLE 6. Analysis Results Relative to Those for Steel Frames

Frame	k_{ini} , kN/cm	F_u , kN	$\delta_{1,u}$, cm	$\delta_{2,u}$, cm	$\delta_{3,u}$, cm	$\delta_{4,u}$, cm	μ
With bracings $S = 2$ cm ²	24	48	8.1	8.1	7.3	7.2	5.21
5 cm ²	65	116	15.7	15.6	14.8	14.6	9.15
10 cm ²	93	215	16.5	16.4	15.6	15.4	8.84
20 cm ²	122	244	1.4	1.3	0.8	0.6	—
Fully restrained at the base	0.4	10	27.0	27.0	8.9	8.8	—
Continuous frame	3	31	35.2	35.2	19.5	19.4	3.02

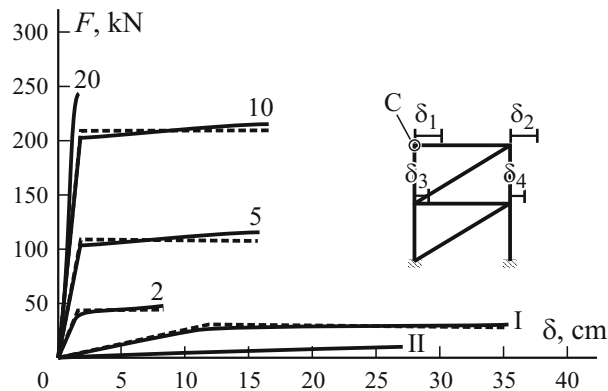


Fig. 18. Actual (—) and idealized (---) pushover curves of a steel frame with the different cross sections of bracings (cm², number at the curves) and of the continuous (I) frame and the frame fully restrained at the base (II).

4.3. Comparison with a steel frame

A pushover analysis for a similar steel frame was also carried out. The steel frame was dimensioned for the same distributed vertical loads as for the pultruded frames. The same three static schemes (Fig. 14) were considered. The beams and columns had HE120A profiles. The cross-sectional areas of bracings were varied from 2 to 20 cm². An elastic-ideally plastic material behavior with the von Mises yield criterion was assigned to all structural elements (Fig. 17). For bracings, the absence of stiffness in compression, induced by the buckling phenomenon, was taken into account. The characteristics of structural elements are given in Table 5.

Results of the pushover analyses are reported in Table 6, and the pushover curves are represented in Fig. 18. As expected, with increasing cross-sectional dimensions of bracings, the stiffness and ultimate bearing capacity of the frames grew. The steel frames, except those with 20-cm² bracings, exhibited a high overall ductility, as expected.

In Figs. 19 and 20, the pushover curves for GFRP and steel braced and moment-resisting frames are compared. As seen in Fig. 19, at the same cross-sectional area of bracings, the steel frame is much stiffer than the pultruded one with respect to the

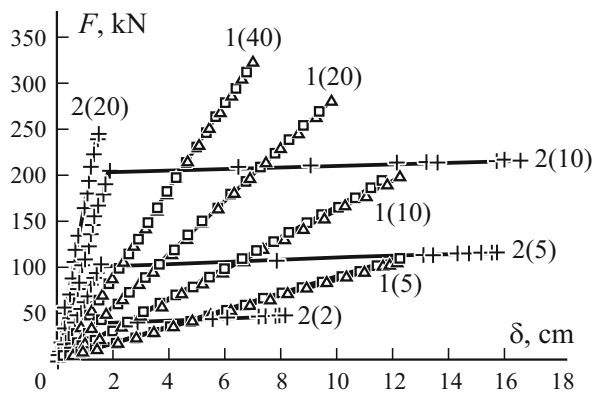


Fig. 19. Comparison between the pushover curves of GFRP (1) and of steel (2, +) frames with TC1 (□) and TC2 (Δ) joints at different cross sections of bracings (cm², numbers at the curves).

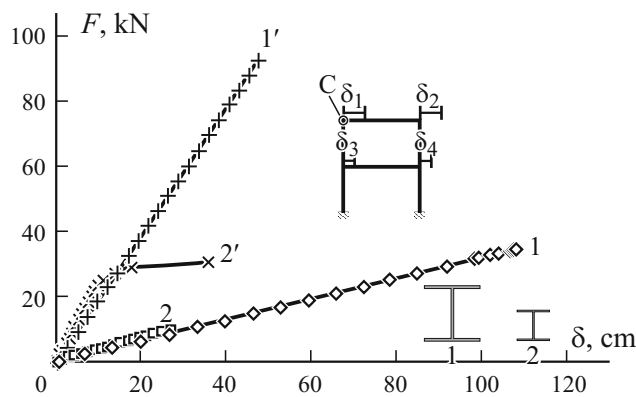


Fig. 20. Comparison between the pushover curves of moment resisting GFRP (1) and steel (1) frames fully restrained at the base and of continuous GFRP (1') and steel (2') frames.

horizontal actions. For the moment-resisting frames (Fig. 20), the initial stiffness of the GFRP and steel ones is approximately the same, while the ultimate displacement and bearing capacity of the GFRP frames are significantly greater.

5. Concluding Remarks

With the aim of evaluating the available overall ductility of FRP pultruded frames, their pushover analyses were carried out based on the hypothesis of the dissipation capacity of the structure concentrated in its joints due to their nonlinear behavior induced by progressive damage.

Proceeding from results of the analyses, the following conclusions can be drawn.

- The braced pultruded frames did not exhibit significant ductility despite the dissipation capacity induced by the nonlinear behavior of its joints. A nonlinear behavior and a related dissipation capacity, although quiet constrained, was observed only in the pultruded frames without bracings. But these frames showed too low values of stiffness and bearing capacity with respect to horizontal actions to be considered as a valid structural solution, at least for seismic designs.

- The behavior of the frames modeled with the actual properties of joints derived from experimental results available in the literature was very close to that of hinged frames. The behavior of braced frames with respect to horizontal actions was determined mainly by the presence of bracings, but the behavior of joints did not play a significant role.

- The braced pultruded frames considered in the analysis exhibited an elevated resistance to seismic actions. Due to the absence of relevant dissipation capacity, a response modification factor (q or R) equal to 1 should be used in seismic designs. As a consequence, higher values of the design seismic accelerations compared with those of structures possessing a significant dissipation capacity, such as steel ones, can be obtained.
- The stiffness and the bearing capacity of the braced frames with respect to horizontal actions were significantly higher than those of moment-resisting frames.
- All pultruded frames with bracings failed either by the ultimate rotation of beam-column joints or by reaching the ultimate tensile strength of bracings, showing a linearly elastic behavior up to failure. The moment-resisting frames collapsed by achieving the ultimate bending moment at the base of columns.
- A comparison similar steel frames as expected, pointed to a higher overall ductility of the latter.
- The braced steel frames exhibited a higher stiffness than the GFRP ones with respect to horizontal actions. As pertains the moment-resisting frames, the stiffness of steel structures was very similar to that of GFRP ones, but the ultimate bearing capacity of pultruded frames was significantly higher than that of steel frames.
- The pushover analysis, even if carried out for different frames in their plane, could also be considered helpful in the three-dimensional case if a regular shape of the frames in plan and elevation is supposed.

REFERENCES

1. J. T. Mottram, "Does performance-based design with FRP components and structures provide any new benefits and challenges?," *Structural Engineer*, **89**, No. 6, 23-27 (2011).
2. L. C. Bank, *Composites for Construction-Structural Design with FRP Materials*, John Wiley & Sons, N.J. (2006).
3. S. Russo, "Experimental and finite element analysis of a very large pultruded FRP structure subjected to free vibration," *Compos. Struct.*, **94**, No. 3, 1097-1105 (2012).
4. EC8, Eurocode No 8. Design of structures for earthquake resistance, European Committee for standardization, EN 1998-1:2005 (2001).
5. M. Mahmoudi and M. Zaree, "Evaluating response modification factors of concentrically braced steel frames," *J. Construct. Steel Research*, **66**, No. 10, 1196-1204 (2010).
6. B. Asgarian and H. R. Shokrgozar, "BRBF response modification factor," *J. Construct. Steel Research*, **65**, No. 2, 290-298 (2009).
7. J. Kim and H. Choi, "Response modification factors of chevron-braced frames," *Engineering Structures*, **27**, No. 2, 285-300 (2005).
8. T. Genshu and Z. Yongfeng, "Seismic force modification factors for modified-Clough hysteretic model," *Engineering Structures*, **29**, No. 11, 3053-3070 (2007).
9. Y. Lu, H. Hao, P. G. Carydis, and H. Mouzakis, "Seismic performance of RC frames designed for three different ductility levels," *Engineering Structures*, **23**, No. 5, 537-547 (2001).
10. B. Borzi and A. S. Elnashai, "Refined force reduction factors for seismic design," *Engineering Structures*, **22**, No. 10, 1244-1260 (2000).
11. C. P. Providakis, "Pushover analysis of base-isolated steel-concrete composite structures under near-fault excitations," *Soil Dynamics and Earthquake Engineering*, **28**, No. 4, 293-304 (2008).
12. M. R. Maheri and R. Akbari, "Seismic behaviour factor, R , for steel X-braced and knee-braced RC buildings," *Engineering Structures*, **25**, No. 12, 1505-1513 (2003).
13. M. R. Maheri, R. Kousari, and M. Razazan, "Pushover tests on steel X-braced and knee-braced RC frames," *Engineering Structures*, **25**, No. 13, 1697-1705 (2003).
14. D. A. Foutch and S. Y. Yun, "Modeling of steel moment frames for seismic loads", *J. Construct. Steel Research*, **58**, No. 5-8, 529-564 (2002).

15. H. Moghaddam and I. Hajirasouliha, "An investigation on the accuracy of pushover analysis for estimating the seismic deformation of braced steel frames," *J. Construct. Steel Research*, **62**, No. 4, 343-351 (2006).
16. L. DiSarno, A. S. Elnashaib, and D. A. Nethercote, "Seismic response of stainless steel braced frames," *J. Construct. Steel Research*, **1**, No. 64, 914-925 (2008).
17. G. E. Thermou, A. S. Elnashai, A. Plumier, and C. Doneux, "Seismic design and performance of composite frames," *J. Construct. Steel Research*, **60**, No. 1, 31-57 (2004).
18. M. Izadinia, M. A. Rahgozar, and O. Mohammadrezaei, "Response modification factor for steel moment-resisting frames by different pushover analysis methods," *J. Construct. Steel Research*, **79**, 83-90 (2012).
19. E. F. Gray, H. C. Browne, W. Burkhardt, T. J. Fowler, A. Lizzio, J. F. I. McDermott, et al., *Structural Plastics Design Manual, Manuals and Reports on Engineering Practice*, American Society of Civil Engineers (1984).
20. S. Russo, "Buckling of GFRP pultruded columns," *Proc. of the Int. Conf. Composite in Construction, CCC2001, Porto, Portugal, 10-12 October 2001* (2001).
21. A. Di Tommaso and S. Russo, "Shape influence in buckling of GFRP pultrudes columns," *Mech. Compos. Mater.*, **39**, No. 4, 329-340 (2003).
22. S. Russo, "Performance of a PFRP structure covering a historic building struck by an earthquake," *Proc. the 5th Int. Conf. Advanced Composites in Construction 2011*, 51-57 (2011).
23. S. Russo and A. Adilardi, "Innovative design approach to a GFRP pedestrian bridge: Structural aspects, engineering optimization and maintenance," *Proc. The Fifth Int. Conf. on Bridge Maintenance, Safety and Management, Philadelphia (USA), 11-15 July 2010*, 2455-2459 (2010).
24. G. Boscato and S. Russo, "On mechanical performance of different type of FRP beams as reinforcement of pedestrian bridge," *Bridge Maintenance, Safety Management, Health Monitoring and Informatics: Proc. the Fourth Int. Conf. on Bridge Maintenance, Safety and Management, Seoul, Korea, July 13-17, 2008* (2008).
25. G. Boscato, C. Casalegno, S. Russo, and J. T. Mottram, "Buckling of built-up columns of pultruded fiber-reinforced polymer C-sections," *J. Compos. for Construct.*, **18**, No. 4, (2014).
26. G. Boscato, C. Casalegno, S. Russo, and J. T. Mottram, "Buckling of GFRP pultruded built-up columns," *Proc. Advanced Composites in Construction Conf. 2013, Queen's University Belfast, UK*, pp. 178-189 (2013).
27. S. Russo, "Damage assessment of GFRP pultruded structural elements," *J. Compos. Struct.*, **96**, 661-669 (2013).
28. G. Boscato and S. Russo, "Free vibrations of pultruded FRP elements: Mechanical characterization, analysis, and applications," *J. Compos. for Construct.*, **13**, No. 6, 565-574 (2009).
29. G. Boscato and S. Russo, "Free vibrations of a pultruded GFRP frame with different rotational stiffnesses of bolted joints," *Mech. Compos. Mater.*, **48**, No. 6, pp. 655-668 (2013).
30. G. Boscato, J. T. Mottram, and S. Russo, "Dynamic response of a sheet pile of fiber-reinforced polymer for waterfront barriers," *J. Compos. for Construct.*, **15**, No. 6, 974-984 (2011).
31. C. Casalegno and S. Russo, "FE progressive failure analysis of all-GFRP pultruded beam-column bolted joints," *Composites: Mechanics, Computations, Applications. An Int. J.*, **5**, No. 3, 1-21 (2014).
32. L. C. Bank and A. S. Mosallam, "Creep and failure of a full-size fiber-reinforced plastic pultruded frame," *Composites Engineering*, **2**, No. 3, 213-227 (1992).
33. A. S. Mosallam and L. C. Bank, "Short-term behavior of pultruded fiber-reinforced plastic frame," *J. Struct. Engineering*, **118**, No. 7, 1937-1954 (1992).
34. TNO Diana, *Diana - Finite Element Analysis User's Manual, Release 9.4*, TNO Diana (2010).
35. Creative Pultrusions I, *The Pultex® Pultrusion Design Manual of Standard and Custom Fiber Reinforced Polymer Structural Profiles* (2004).
36. Top Glass Technical data – Material properties Triglass™ profiles, Top Glass SPA, www.topglass.it (2014).
37. G. J. Turvey and C. Cooper, "Review of tests on bolted joints between pultruded GRP profiles," *Proc. the Institution of Civil Engineers: Structures and Buildings*, **157**, No. 3, 211-233 (2004).
38. J. T. Mottram and Y. Zheng, "State-of-the-art review on the design of beam-to-column connections for pultruded frames," *Compos. Struct.*, **35**, No. 4, 387-401 (1996).

39. G. J. Turvey and C. Cooper, "Semi-rigid column-base connections in pultruded GRP frame structures," *Computers and Structures*, **76**, No. 1, 77-88 (2000).
40. A. S. Mosallam, *Design guide for FRP composite connections*, ASCE Manuals and Reports on Engineering Practice, No.102, Am. Soc. of Civil Engineers (2011).
41. A. J. Bass and J. T. Mottram, "Behaviour of connections in frames of fibre reinforced polymer section," *Structural Engineer*, **72**, No. 17, 280-285 (1994).
42. J. T. Mottram and Y. Zheng, "Further tests on beam-to-column connections for pultruded frames: Web-cleated", *J. Compos. for Construct.*, **3**, No. 1, 3-11 (1999).